Operation and Design Principles of Biological Molecular Machines

Department of Life and Coordination-Complex Molecular Science
Division of Biomolecular Functions

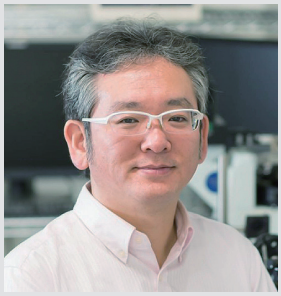

IINO, Ryota
Professor
[iino@ims.ac.jp]

Education
1995 B.E. Kyoto University
1997 M.E. Kyoto University
2003 Ph.D. Nagoya University

Professional Employment
2000 Research Associate, Japan Science and Technology Cooperation
2002 Research Associate, Japan Science and Technology Agency
2005 Specially-Appointed Assistant Professor, Osaka University
2006 Assistant Professor, Osaka University
2011 Lecturer, The University of Tokyo
2013 Associate Professor, The University of Tokyo
2014 Professor, Institute for Molecular Science
Professor, Okazaki Institute for Integrative Bioscience (–2018)
Professor, The Graduate University for Advanced Studies

Award
2012 Emerging Investigator. Lab on a Chip., The Royal Society of Chemistry, U.K.

Member
Assistant Professor
OTOMO, Akihiro
Post-Doctoral Fellow
KIM, Ju-Young
KEYA, Jakia Jannat
HARASHIMA, Takanori
MATSUMOTO, Kohsuke
Visiting Scientist
YU, Yan
Technical Fellow
OKUNI, Yasuko
KON, Yayoi
Secretary
NAKANE, Kaori

Keywords Molecular Motors, Single-Molecule Analysis, Protein Engineering

Activity of life is supported by various molecular machines made of proteins. Protein molecular machines are tiny, but show very high performance, and are superior to man-made machines in many aspects. One of the representatives of protein molecular machines is linear and rotary molecular motors (Figure 1). Molecular motors generate mechanical forces and torques that drive their unidirectional motions from the energy of chemical reaction or the electrochemical potential across the cell membrane. We unveil operation principles of molecular motors with advanced single-molecule functional analysis. With the help of site-saturation mutagenesis and robot-based automation, we also engineer non-natural molecular motors to understand their design principles.

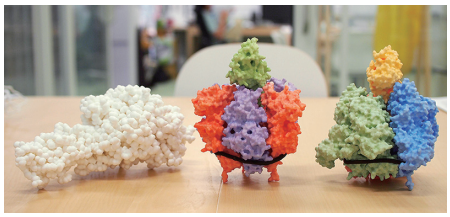

Figure 1. Protein molecular machines. (Left) A linear molecular motor chitinase A. (Center and Right) Rotary molecular motors F_1-ATPase and V_1-ATPase, respectively.

Selected Publications

- A. Nakamura, N. Kobayashi, N. Koga and R. Iino, "Positive Charge Introduction on the Surface of Thermostabilized PET Hydrolase Facilitates PET Binding and Degradation," *ACS Catal.* **11**, 8550–8564 (2021).
- A. Visootsat, A. Nakamura, P. Vignon, H. Watanabe, T. Uchihashi and R. Iino, "Single-Molecule Imaging Analysis Reveals the Mechanism of a High-Catalytic-Activity Mutant of Chitinase A from *Serratia marcescens*," *J. Biol. Chem.* **295**, 1915–1925 (2020).
- J. Ando, T. Shima, R. Kanazawa, R. Shimo-Kon, A. Nakamura, M. Yamamoto, T. Kon and R. Iino, "Small Stepping Motion of Processive Dynein Revealed by Load-Free High-Speed Single-Particle Tracking," *Sci. Rep.* **10**, 1080 (2020).
- J. Ando, A. Nakamura, M. Yamamoto, C. Song, K. Murata and R. Iino, "Multicolor High-Speed Tracking of Single Biomolecules with Silver, Gold, Silver-Gold Alloy Nanoparticles," *ACS Photonics* **6**, 2870–2883 (2019).
- T. Iida, Y. Minagawa, H. Ueno, F. Kawai, T. Murata and R. Iino, "Single-Molecule Analysis Reveals Rotational Substeps and Chemo-Mechanical Coupling Scheme of *Enterococcus hirae* V_1-ATPase," *J. Biol. Chem.* **294**, 17017–17030 (2019).
- J. Ando, A. Nakamura, A. Visootsat, M. Yamamoto, C. Song, K. Murata and R. Iino, "Single-Nanoparticle Tracking with Angstrom Localization Precision and Microsecond Time Resolution," *Biophys. J.* **115**, 2413–2427 (2018).
- A. Nakamura, K. Okazaki, T. Furuta, M. Sakurai and R. Iino, "Processive Chitinase is Brownian Monorail Operated by Fast Catalysis after Peeling Rail from Crystalline Chitin," *Nat. Commun.* **9**, 3814 (2018).
- A. Nakamura, T. Tasaki, Y. Okuni, C. Song, K. Murata, T. Kozai, M. Hara, H. Sugimoto, K. Suzuki, T. Watanabe, T. Uchihashi, H. Noji and R. Iino, "Rate Constants, Processivity, and Productive Binding Ratio of Chitinase A Revealed by Single-Molecule Analysis," *Phys. Chem. Chem. Phys.* **20**, 3010–3018 (2018).

1. Direct Observation of Stepping Rotation of V-ATPase Reveals Rigid Component in Coupling between V_o and V_1 Motors[1)]

V-ATPases are rotary motor proteins that convert the chemical energy of ATP into the electrochemical potential of ions across cell membranes (Figure 2). V-ATPases consist of two rotary motors, V_o and V_1, and *Enterococcus hirae* V-ATPase (EhV_oV_1) actively transports Na^+ in V_o (EhV_o) by using torque generated by ATP hydrolysis in V_1 (EhV_1). Here, we observed ATP-driven stepping rotation of detergent-solubilized EhV_oV_1 wild-type, aE634A, and BR350K mutants under various Na^+ and ATP concentrations ([Na^+] and [ATP], respectively) by using a 40-nm gold nanoparticle as a low-load probe. When [Na^+] was low and [ATP] was high, under the condition that only Na^+ binding to EhV_o is rate-limiting, wild-type and aE634A exhibited 10-pausing positions reflecting 10-fold symmetry of the EhV_o rotor and almost no backward steps. Duration time before the forward steps was inversely proportional to [Na^+], confirming that Na^+ binding triggers the steps. When both [ATP] and [Na^+] were low, under the condition that both Na^+ and ATP bindings are rate-limiting, aE634A exhibited 13-pausing positions reflecting 10- and 3-fold symmetries of EhV_o and EhV_1, respectively (Figure 3). The distribution of duration time before the forward step was fitted well by the sum of two exponential decay functions with distinct time constants. Furthermore, occasional backward steps smaller than 36° were observed. Small backward steps were also observed during three long ATP cleavage pauses of BR350K. These results indicate that EhV_o and EhV_1 do not share pausing positions, Na^+ and ATP bindings occur at different angles, and the coupling between EhV_o and EhV_1 has a rigid component (Figure 4).

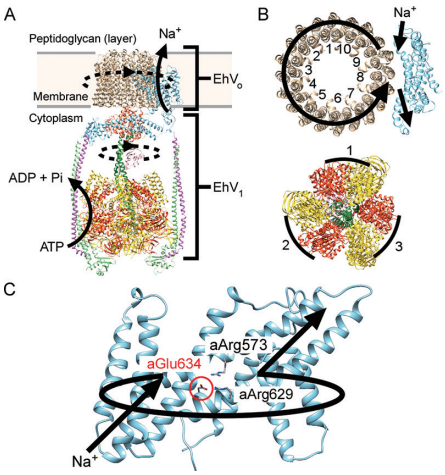

Figure 2. (A) Overall architecture of EhV_oV_1. The dotted circular arcs represent the rotation direction driven by ATP hydrolysis. (B) (top) Top view of a-subunit (cyan) and c_{10}-ring (brown) of EhV_o and (bottom) A- (yellow), B- (orange), D- (green), and F-subunits (pink) of EhV_1. The black arrow at the top indicates the path of Na^+ movement during ATP-driven rotation. The arcs at the bottom represent the catalytic AB pairs. (C) Side view of a-subunit viewed from the c-subunit. The mutated residue, aGlu634, is located on the surface of the entry half-channel of the a-subunit as highlighted in red letters and a circle.

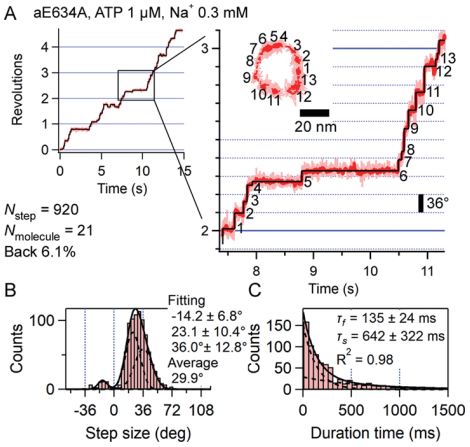

Figure 3. (A) Typical trajectory of rotation at 1 μM ATP and 0.3 mM Na^+ recorded at 1,000 fps. Enlarged view of one revolution (360°) is shown on the right. Pink, red, and black traces represent raw, median-filtered (current ± 7 frames), and fitted trajectories, respectively. The inset shows the corresponding *x*-*y* trajectory. Pink lines and red dots represent the raw and median-filtered (current ± 7 frames) coordinates, respectively. (B) Distribution of the step size fitted with the sum of three Gaussians: One peak in backward (minus) direction and two peaks in forward (plus) direction, one of which was fixed at 36°, assuming that it was the step of EhV_o. (C) Distribution of the duration time before the forward step fitted with the sum of two exponential decay functions.

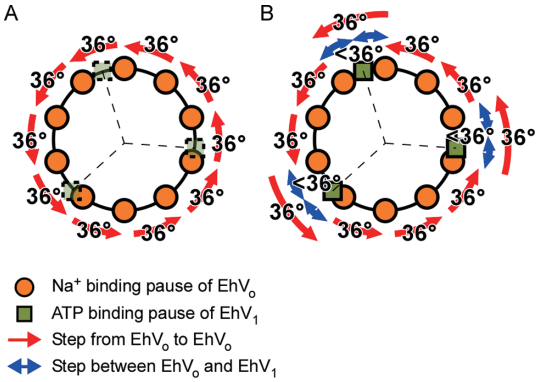

Figure 4. Schematic models of the stepping rotation and rigid coupling of EhV_oV_1. The orange circles and dark green squares indicate the pausing positions waiting for Na^+ binding to EhV_o and ATP binding to EhV_1, respectively. The red arrows indicate the 36° steps between adjacent pausing positions for the EhV_o. The blue arrows indicate the backward and forward steps smaller than 36° between adjacent pausing positions for EhV_o and EhV_1. (A) Condition in which only Na^+ binding to EhV_o is rate-limiting. In this condition, the pauses waiting for ATP binding to EhV_1 are too short to be detected, and EhV_oV_1 rotates unidirectionally without backward steps. (B) Condition in which both Na^+ and ATP bindings are rate-limiting. The pausing positions waiting for ATP binding are visualized, and then 13-pausing positions are detected per single turn. Because no torque is generated during the pauses waiting for ATP binding to EhV_1, EhV_oV_1 rotates to the backward and forward pausing positions of EhV_o driven by Brownian motion.

Reference

1) A. Otomo, T. Iida, Y. Okuni, H. Ueno, T. Murata and R. Iino, *bioRxiv* DOI: 10.1101/2022.06.13.494302 (2022).